ISBN: 978-3-95450-215-8 ISSN: 2226-0366 doi:10.18429/JACoW-LINAC2022-THPOJO10

RF DESIGN AND CHARACTERISATION OF THE CLARA 10HZ GUN WITH PHOTOCATHODE LOAD/LOCK UPGRADE

A. J. Gilfellon*, L. S. Cowie †, B. L. Militsyn ‡, T. J. Jones, R. Valizadeh,
STFC, Daresbury Laboratory, UK.

Abstract

The 2.5 cell, S-band, 10Hz repetition rate electron gun (**Gun-10**) for the CLARA (**C**ompact **L**inear **A**ccelerator for **R**esearch and **A**pplications) accelerator underwent an upgrade during the scheduled shutdown period in the summer of 2019. The existing single photocathode/back plate component was replaced by a back plate with an integrated load/lock system capable of rapid exchanges of photocathode plugs. Here we outline the motivation and RF design of the back plate and also detail the RF testing and characterisation of the upgraded gun in terms of the unloaded quality factor, Q_0, the RF power coupling match, β, the percent field flatness and the operating frequency of the cavity, calculated from the frequency measured in the laboratory. Finally, via simulations, a square root of the forward power, $\sqrt{P_F}$, vs. beam momentum plot was produced that we predict the gun will deliver once it goes back online.

INTRODUCTION

The need to change photocathodes arises from the degradation of the cathode's Quantum Efficiency over time, damage from the photoinjector laser and RF breakdown. CLARA photocathode exchanges have occurred approximately every 6 - 12 months. In the previous configuration, where the removable backplate of the gun also functioned as the photocathode, any exchange was invasive and time consuming (~ 3 weeks). The main motivations for the 10 Hz gun back plate upgrade, therefore, were:

- Exchanges can be carried out much more rapidly in-situ , ~30 minutes.
- Exchanges can take place under vacuum conditions.
- Eliminate the risk of an oxide layer forming on the cathode surface.
- Remove the need for lengthy RF reconditioning.
- Achieve more stable and repeatable RF characteristics during a cathode load and between load events.

In the following sections we highlight some of the RF concerns that went into the design of the upgrade, the post-upgrade characterisation of Gun-10 in terms of Q_0, β, percent field flatness and the operating frequency. Finally we determine by how much the working surface of the photocathode is intruding on the internal space of the gun, cathode penetration, which is the first step in constructing the $\sqrt{P_F}$, vs. beam momentum plot that we predict Gun-10 will deliver.

* anthony.gilfellon@stfc.ac.uk
† louise.cowie@stfc.ac.uk
‡ boris.militsyn@stfc.ac.uk

RF DESIGN

The introduction of a load/lock photocathode system into Gun-10 was not as simple as replacing the original cathode with a flat plate and a plug.

If the upgraded backplate was simply fitted in the same position as the original design, key RF parameters would change considerably, see table 1 for a comparison of simulated results between the original and a simple backplate replacement design.

In order to preserve the RF character of the cavity the majority of the cathode surface was recessed 300 µm further back than the pre-upgrade Gun-10 cathode. Contact between the upgraded backplate and the cavity wall includes a 300 µm step, which is 40 mm from the cavity centre. The step is rounded with a radius of 150 µm on both 90° angles. The centre of the step is at 40 mm radius, and the step extends from 39.85 mm to 40.15 mm. See Fig. 1 for the general design.

Table 1: A comparison of simulated results for the pre-upgrade design and the simple load/lock replacement design that shows how the RF characteristics would change and highlights the need for a more nuanced design approach.

Mode	Stat.	Original Cathode	Upgraded Cathode
π	freq. (GHz)	2.99863	2.99908
	β	1.03	0.61
	Q_0	12302	11270
$3\pi/5$	freq. (GHz)	2.99550	2.99617
	β	0.81	1.5
	Q_0	11093	11282
$\pi/5$	freq. (GHz)	2.99048	2.99103
	β	1.228	0.272
	Q_0	11108	11846

RF CHARACTERISATION

General Procedure

Once the backplate was fixed in its optimal position and the specially made dummy beadpull photocathode plug with an on-axis hole for the thread to pass through was installed, the beadpull experiments could begin. The perturbation

ISBN: 978-3-95450-215-8 ISSN: 2226-0366 doi:10.18429/JACoW-LINAC2022-THPOJO10

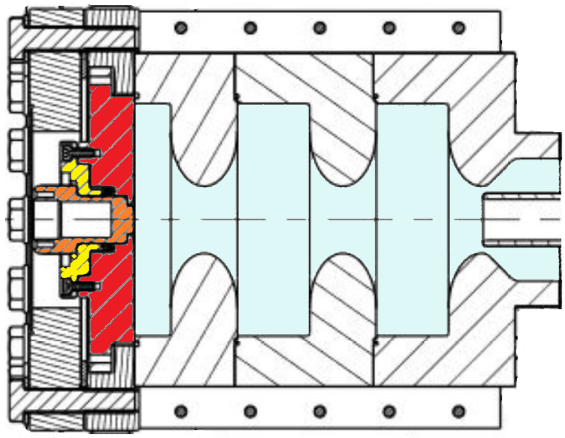

Figure 1: A schematic of the design that was put forward and implemented. The coloured components are **pale blue**; the 2.5 s-band RF cells; **red**; the solid copper back plate, **yellow**; the spring loaded photocathode plug holder, **orange**; the photocathode plug.

theory underpinning beadpull experiments is well described by [1]. The four-stage beadpull procedure was:

1. record the pre-beadpull frequency vs. phase data,
2. a real-time recording of the bead travelling from the beam pipe to the dummy beadpull cathode in terms of time vs. real & imaginary components of the S11 reflection coefficient, Γ,
3. as step 2, but with the bead travelling from the cathode to the back of the beam pipe,
4. record the post-beadpull frequency vs. phase data.

The requirement to record the pre- and post beadpull frequency vs. phase data is to ensure that any phase drift linked to thermal drift was negligible, or at least linear so the data could be detrended appropriately. The data analysis method that returns the RF power coupling factor, β and the cavity's quality factor, Q_0 was taken from [2] and is outlined here. Firstly, β was calculated for each measurement using Γ_{min} and Γ_{max}, the minimum and maximum $|\Gamma|$ values, where

$$|\Gamma| = \sqrt{\Re(\Gamma)^2 + \Im(\Gamma)^2}, \quad (1)$$

is the magnitude of the reflection coefficient and

$$\beta = \frac{\Gamma_{max} - \Gamma_{min}}{\Gamma_{max} + \Gamma_{min}}. \quad (2)$$

if the cavity is under-coupled, or

$$\beta = \frac{\Gamma_{max} + \Gamma_{min}}{\Gamma_{max} - \Gamma_{min}}. \quad (3)$$

if the cells are over-coupled. The frequency at which Γ_{min} occurred was recorded as the resonant frequency of the cavity which was then used to calculate the cavity frequency under operating conditions.

The loaded quality factor, Q_L was determined by

$$Q_L = \frac{f_0}{f_1 - f_2}, \quad (4)$$

where f_1 and f_2 are the frequencies where $\Im(\Gamma)$ is at a maximum and minimum respectively, while f_0 is the frequency at which $|\Gamma|$ is a minimum.

Finally the unloaded quality factor of the cavity, Q_0 is calculated by

$$Q_0 = (1 + \beta) Q_L. \quad (5)$$

Stability & Repeatability

We then investigate the stability of each RF statistic during a single load as well as the repeatability between loads. The cathode was unloaded and loaded six times with four beadpulls recorded for each separate loading of a molybdenum cathode. See Fig. 2 and table 2 for the results. A possible reason for variations within the same cathode load could be differing degrees of contact between the cathode plug shoulder and the gun's backplate, whereas variation between cathode loads could be the result of small changes in atmospheric conditions.

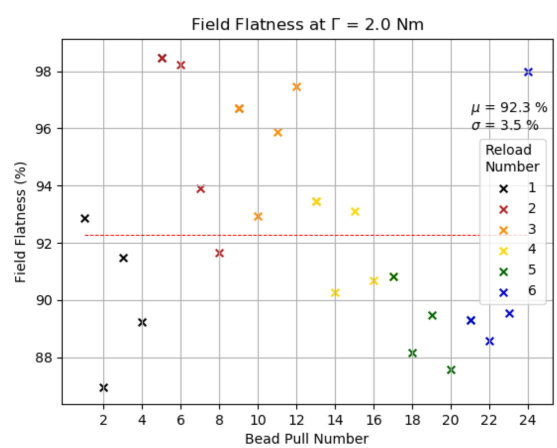

Figure 2: A plot of the calculated field flatness of the 10Hz gun for each beadpull, each colour represents a different load event. The mean average field flatness is (92.3 ± 3.5)%.

Table 2: The Inverse Variance Weighted Means and their Errors from the Results of the Gun-10 Cathode Unload/Reload Analysis.

Quantity	Weighted mean & uncertainty
Vacuum Freq. (GHz±kHz)	2.998528 ± 1.2
% field flatness	92.3 ± 3.5
Q_0	10902 ± 39

ISBN: 978-3-95450-215-8 ISSN: 2226-0366 doi:10.18429/JACoW-LINAC2022-THPOJO10

SIMULATIONS & PREDICTED BEAM MOMENTUM

The final objective was to determine the beam momentum that the upgraded Gun-10 will be likely to deliver. This was done via a series of simulations using CST Studio Suite [3] and ASTRA in conjunction with the π mode vacuum frequency and Q_0 of the hybrid Mo/Cu photocathode which is likely to be used in Gun-10 when it goes back online, calculated as being 2998.564 MHz and 10537 respectively. The field flatness, vacuum frequency and Q_0 of the gun are very sensitive to the degree to which the photocathode intrudes into the internal cavity space. The nominal position is for the tip of cathode to be flush with the back-plate, however, due to manufacturing errors and baking induced changes to the cathode's dimensions, the actual value of cathode penetration needed to be determined. This was achieved via a CST simulation with an in-built parameter sweep of cathode penetration from −250 microns, via zero to 250 microns. Here, the minus values describe a situation where the puck is shy of being flush with the backplate, which is plausible.

From the results of the simulation, the photocathode was determined to have a penetration value compatible with zero, so the next step was to simulate this situation, again using CST and the values of the E-field along the z-axis as inputs for an axially symmetric ASTRA simulation. A plot of z-coordinate vs. $|E|$, $\Re(E)$ and $\Im(E)$ is shown in Fig. 3. A slight complication with using the CST data as an input for the ASTRA simulation was that the $\Re(E)$ and the $\Im(E)$ were out of phase with each other, leading to a situation where $|E|$ never achieved a zero value, even in the irises, see inserted subplot in Fig. 3. This is an expected aspect of the simulation since there is a travelling wave component in the cavity that was present before the upgrade. ASTRA was able to handle this as an input after the data was scaled appropriately since CST uses a mean RF forward power of 0.5 W and the nominal operating forward RF power of Gun-10 is 8 MW, see Fig. 4 for the ASTRA simulation results.

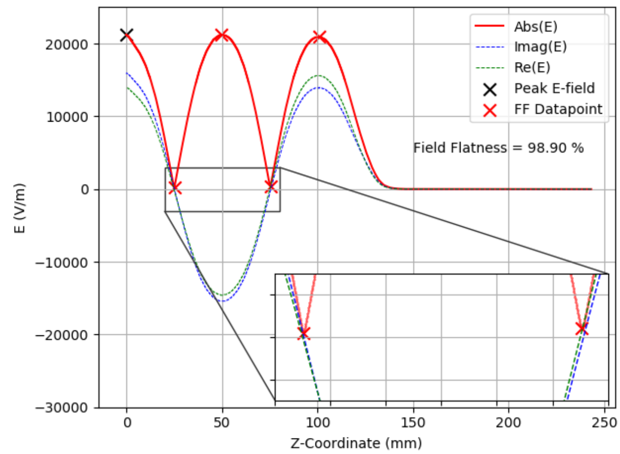

Figure 3: A plot of z-axis coordinate vs. electric field strength in the second CST simulation with nominal cathode penetration. The Peak E-field value and the field flatness were found to be 21.260 kV/m and 98.9% respectively. The inserted subplot highlights the slight travelling wave character of the gun.

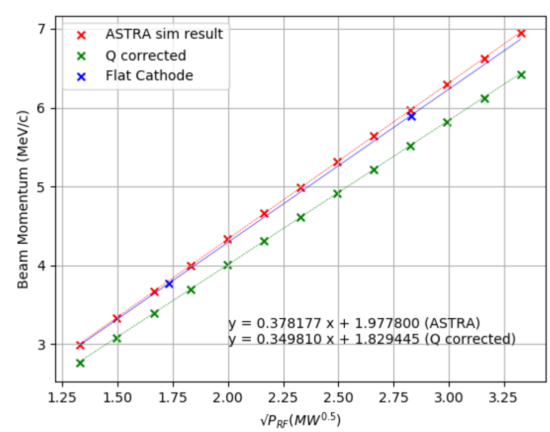

Figure 4: A plot of the square root of forward RF power, $\sqrt{P_{RF}}$ vs. momentum. The red plot shows the results of the ASTRA simulation, while the green shows the same data rescaled by a Q_0 scaling factor; $Q_{0,meas}/Q_{0,sim}$. The blue plot shows the relation for the flat backplate for reference.

CONCLUSION

The stability and repeatability results for the unloading/reloading of the photocathodes were within acceptable bounds.

Simulations were carried out to find the extent to which the run cathode was intruding into the internal space of Gun-10, which impacts on the expected field flatness and consequently the beam momentum. The conclusions reached are that the working face of the Cu puck on the run cathode looks to be flush with the inside of Gun-10 and the predicted beam momentum of Gun-10 using this cathode with a forward RF power of 6 MW is 4.831 MeV/c, which is almost identical to the momentum delivered by the original flat backplate cathode at the same power.

ACKNOWLEDGEMENTS

The authors acknowledge the help of Julian McKenzie on the ASTRA simulations and Research Instruments for use of their "CONVERTF" software application.

REFERENCES

[1] H. Padamsee, J. Knobloch, and T. Hays, *RF superconductivity for accelerators*. Wiley-VCH, 2008.

[2] L. S. Cowie, *Vela gun missing momentum reportv3*, 2016.

[3] https://www.cst.com.